Continuous damage approach in analysis of concrete structures under impulsive load

Krzysztof Cichocki and Mariusz Ruchwa
Technical University of Koszalin, Department of Civil and Environmental Engineering
Raclawicka 15-17, 75-620 Koszalin, Poland
e-mail: kris@tu.koszalin.pl

Abstract

This study analyzes the highly nonlinear shock-wave phenomena in reinforced concrete plates blast loaded by contact detonation of a explosive charge. The response of reinforced concrete to such dynamic loads is of great interest for designing safety facilities. In order to obtain reliable results from numerical analysis, an improved material model for concrete was adopted and implemented into a finite element code. The first part of the paper focuses on the description of the material model, and the second part is devoted to the validation of the assumed model by the numerical simulation of an experimental test, performed by Kraus and Roetzer [6].

Keywords: concrete, material model, blast load

Introduction

A realistic evaluation of the structural response due to blast load is a task of timely and growing importance in many engineering situations, no longer confined to classified areas of defense technology. The growing threat of terrorist attacks, industrial incidents, and transport collisions (cars, airplanes, etc.) must be taken into consideration in the design process, especially for important structures located in areas of possible threat.

In order to obtain reliable results from numerical analysis, the rate - dependent plastic - damage constitutive model for concrete has been applied, based on considerations presented by Faria and Oliver [3]. The main goal of the choice of material model was to obtain the relatively simple algorithm, reliable and easy to implement into commercial finite element computer code. The model has its own point of departure on the continuum damage mechanics [5, 7], which is a very powerful and consistent theory that is based on the thermodynamics of irreversible processes. Nonlinear mechanisms of degradation of concrete under tensile or compressive loading conditions are characterized by two independent scalar internal damage variables. This option deals with tensile and compressive concrete behavior in a unified fashion, where the same material model is adopted for any load combinations. Rate dependency, a very important factor in analysis of blast loaded structures, has been accounted for as an almost natural extension to the plastic-damage model, introducing a viscous regularization of the evolution laws for the damage variables.

The assumed material model has been implemented into the computer code Abaqus/Explicit [1], as a user subroutine. In order to verify the assumed material model numerical simulation of the experimental test performed by Kraus and Roetzer [6] has been carried out. In this experiment, the permanent damages developed in a thick plate by a contact explosion of various PETN charges were examined. Due to the relatively significant thickness of the plate, the effects of the wave propagation in the direction perpendicular to the plate surface have also been observed.

Load due to the explosion has been modeled as a field of pressure, variable in time and space. For such simple geometry, consisting of the relatively rigid flat surface loaded by a contact explosion, Henrych's [4] empirical formula was introduced. This approach is only applicable for rather simple geometry structures, where the effects of blast wave reflection and their consequent interaction are not so significant [2].

Material model for concrete

The applied material model is based on the effective stress concept [7], and the hypothesis of the stress equivalence [8]. An expression for the effective stress tensor has assumed the following form:

$$\bar{\boldsymbol{\sigma}} = \mathbf{D}_0 : \left(\boldsymbol{\varepsilon} - \boldsymbol{\varepsilon}^{\mathbf{p}}\right) \tag{1}$$

where $\mathbf{D_0}$ is the fourth order linear-elastic constitutive matrix, $\boldsymbol{\varepsilon}$ is the second order strain tensor, $\boldsymbol{\varepsilon}^p$ is the plastic strain tensor.

The following form of the Helmholtz free energy potential has been adopted:

$$\begin{aligned}\Psi(\boldsymbol{\varepsilon},\boldsymbol{\varepsilon}^p,d^+,d^-) &= (1-d^+)\Psi_0^+(\boldsymbol{\varepsilon},\boldsymbol{\varepsilon}^p) + \\ &+ (1-d^-)\Psi_0^-(\boldsymbol{\varepsilon},\boldsymbol{\varepsilon}^p)\end{aligned} \tag{2}$$

The elastic free energies are defined as follows:

$$\begin{aligned}\Psi_0^+ &= \frac{1}{2}\bar{\boldsymbol{\sigma}}^+ : \mathbf{D}_0^{-1} : \bar{\boldsymbol{\sigma}} \\ \Psi_0^- &= \frac{1}{2}\bar{\boldsymbol{\sigma}}^- : \mathbf{D}_0^{-1} : \bar{\boldsymbol{\sigma}}\end{aligned} \tag{3}$$

d^+, d^- are the damage variables, assigned respectively to compression and tension. Their values are of the range <0,1>. The split of the effective stress tensor $\bar{\boldsymbol{\sigma}}$ into tensile and compressive parts according to [3] gives adequately the $\overline{\sigma}^{+}$ and $\overline{\sigma}^{-}$.

In order to characterize the scalar damage, a concept of equivalent effective compressive and tensile stress has been introduced. In the present work, they will assume the following forms:

$$\overline{r}^{+} = \sqrt{\overline{\boldsymbol{\sigma}}^{+} : \mathbf{D}_{0}^{-1} : \overline{\boldsymbol{\sigma}}^{+}}$$
$$\overline{r}^{-} = \sqrt{\sqrt{3}\,(K\overline{\sigma}_{\text{oct}}^{-} + \overline{\tau}_{\text{oct}}^{-})} \tag{4}$$

K is a material constant, and the $\overline{\sigma}_{\text{oct}}^{-}, \overline{\tau}_{\text{oct}}^{-}$ are the octahedral normal stress and the octahedral shear stress, calculated from $\overline{\sigma}^{-}$.

On the basis of calculated effective equivalent stresses, two damage criteria have been introduced:

$$g^{+}(\overline{r}^{+}, r^{+}) = \overline{r}^{+} - r^{+} \leq 0$$
$$g^{-}(\overline{r}^{-}, r^{-}) = \overline{r}^{-} - r^{-} \leq 0 \tag{5}$$

where the entities r^{+} and r^{-} are current damage thresholds, and control the size of damage surfaces.

The rates of tensile and compressive variable are defined as follows:

$$\dot{d}^{+} = \dot{\overline{r}}^{+} \frac{\partial G^{+}(\overline{r}^{+})}{\partial \overline{r}^{+}} = \dot{G}^{+} \geq 0$$
$$\dot{d}^{-} = \dot{\overline{r}}^{-} \frac{\partial G^{-}(\overline{r}^{-})}{\partial \overline{r}^{-}} = \dot{G}^{-} \geq 0 \tag{6}$$

G^{+}, G^{-} are the appropriate monotonically increasing functions to obtain values of damage variables in the range of <0,1>.

Development of the plastic strain tensor is assumed to have the direction of the elastic strain tensor:

$$\dot{\boldsymbol{\varepsilon}}^{p} = A(\dot{d}^{-}) \frac{\langle \overline{\boldsymbol{\sigma}} : \dot{\boldsymbol{\varepsilon}} \rangle}{\overline{\boldsymbol{\sigma}} : \overline{\boldsymbol{\sigma}}} \mathbf{D}_{0}^{-1} : \overline{\boldsymbol{\sigma}} \tag{7}$$

where A is a material-dependent function, controlling the rate intensity of plastic deformation and preventing plastic evolution during compressive unloading.

The evolution of damage variables has been assumed in the following form, taking into account the different mechanisms of compression and tension damage:

$$d^{+} = 1 - \frac{r_{0}^{+}}{\overline{r}^{+}} e^{A^{+}\left(1 - \frac{\overline{r}^{+}}{r_{0}^{+}}\right)}$$
$$d^{-} = 1 - \frac{r_{0}^{-}}{\overline{r}^{-}}(1 - A^{-}) - A^{-} e^{B^{-}\left(1 - \frac{\overline{r}^{-}}{r_{0}^{-}}\right)} \tag{8}$$

where $A^{+}, A^{-}, B^{-}, r_{0}^{+}, r_{0}^{-}$ are the material constants, described by Yankelevsky et al. [9, 10].

The viscous-damage evolution laws according to Simo and Ju [8] have the following form:

$$\dot{d}^{+} = \frac{\vartheta^{+}}{(f_{u}^{+})^{a^{+}/2}} \langle \overline{r}^{+} - r^{+} \rangle^{a^{+}} \frac{\partial G^{+}(\overline{r}^{+})}{\partial \overline{r}^{+}}$$
$$\dot{r}^{+} = \frac{\vartheta^{+}}{(f_{u}^{+})^{a^{+}/2}} \langle \overline{r}^{+} - r^{+} \rangle^{a^{+}}$$
$$\dot{d}^{-} = \frac{\vartheta^{-}}{(f_{u}^{-})^{a^{-}/2}} \langle \overline{r}^{-} - r^{-} \rangle^{a^{-}} \frac{\partial G^{-}(\overline{r}^{-})}{\partial \overline{r}^{-}}$$
$$\dot{d}^{-} = \frac{\vartheta^{-}}{(f_{u}^{-})^{a^{-}/2}} \langle \overline{r}^{-} - r^{-} \rangle^{a^{-}} \tag{9}$$

In foregoing equations, $\vartheta^{+}, \vartheta^{-}$ are so-called concrete fluidity parameters, and a^{+}, a^{-} are the exponents.

For the reinforcement, the classic von Mises elastoplastic formulation for steel has been adopted, with rate-dependent assumption according to Cowper and Symonds [1].

3. Experimental study

This study has been carried out by Kraus and Roetzer, and is described in detail elsewhere [6]. The test specimen consisted of a simply supported plate with the dimensions 2.0 x 2.0 x 0.3 m. The concrete compressive strength was 46 MPa and the plate was reinforced with 16 mm steel bars (yield stress – 500 MPa) distributed in both directions with 150 mm spacing.

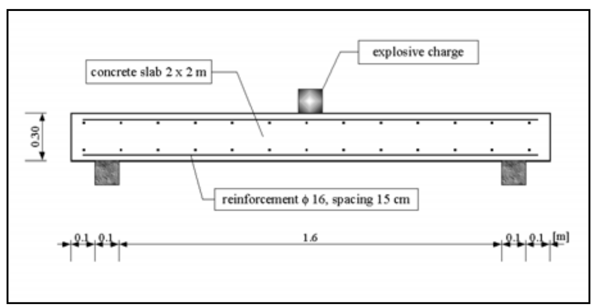

Figure 1. Experimental test setup [6]

Explosive masses of 0.5 kg and 1.0 kg were used. The explosive type is PETN, with a density of 1500 kg/m^{3}. The explosive was formed as a cube, positioned at the center of the slab and detonated. After each test, the plate was cleaned, all debris removed, and the hole volumes and shapes created by the detonation were measured and recorded. Finally, the plates were cut exactly along a vertical plane of symmetry, allowing the crater shapes, the status of the material, and any cracks in the interior of the slab to be evaluated.

The resulting shape of the upper surface crater for 0.5 kg of PETN is shown in Figure 2 and 3. Similar results for the 1.0 kg charge are presented in Figures 4 and 5.

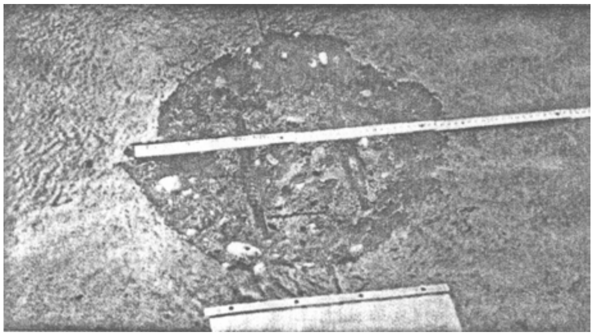

Figure 2. Upper crater for 0.5 kg charge.

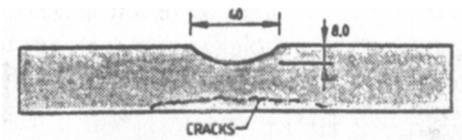

Figure 3. Schematic transverse section of the slab (0.5 kg charge)

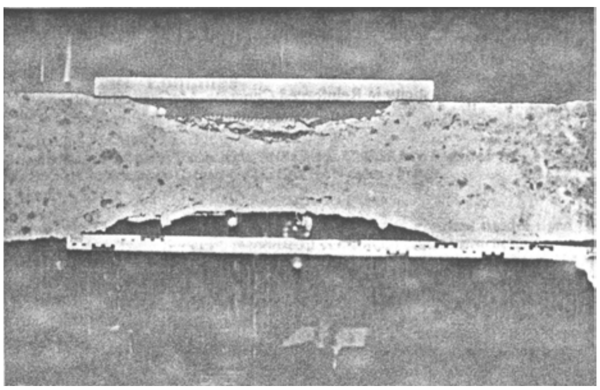

Figure 4. Transverse section of the slab (1.0 kg charge)

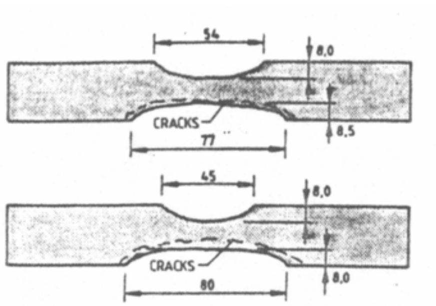

Figure 5. Schematic transverse section of the slab in both directions (1.0 kg charge).

The contact explosion of 0.5 kg charge of PETN produced the upper crater of a diameter 40 cm and depth 8 cm. There were also accumulated cracks in the bottom part of the slab, but without material separation. Contact explosion of 1.0 kg PETN charge created craters on both sides of the slab. Due to the highly random process of the explosion, both craters are asymmetrical, with an approximately circular shape (upper crater: diameter 54-45 cm, depth 8 cm, bottom crater: diameter 77-80 cm, depth 8 cm).

4. Numerical simulation of the experimental test

After the implementation of material model described in this paper into ABAQUS/Explicit code, the crucial factor for the analysis was to assume a representative description of the load produced during the explosion of a charge. The following empirical equations were applied, according to Henrych's [4] empirical study:

In this description, the value of maximum incident pressures Δp_{Φ} at the distance R [m] from the center of TNT charge W [kg] depends on the parameter:

$$\overline{R} = \frac{R}{\sqrt[3]{W}}; \tag{10}$$

In order to model the contact explosion (i.e., confined from one side), and to simulate the presence of the PETN charge (different from TNT), the adequate correction parameters have been applied, according to considerations given in [4].

Additionally, the duration of overpressure according to Henrych is given by a simple formula:

$$t_{ovp} = \sqrt[3]{W} * 10^{-3}(0.107 + 0.444\overline{R} + 0.264\overline{R}^2 - \\ - 0.129\overline{R}^3 + 0.0336\overline{R}^4) \tag{11}$$

The entire set of functions enables the user to describe the change of overpressure with time (for the established point in space). The distribution of pressure in space and time is plotted in Figure 6. The same function is presented as the contour plot for the specific case considered here in Figure 7.

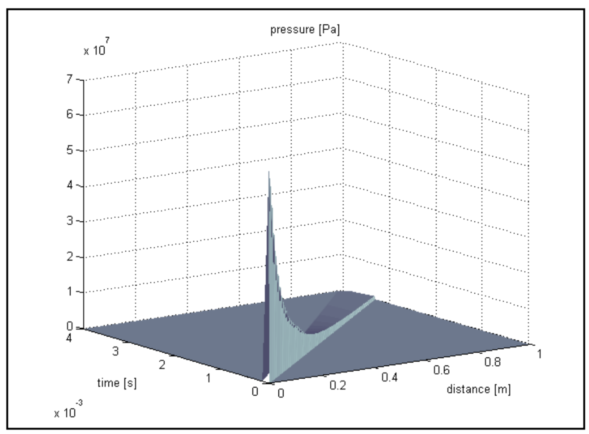

Figure 6. Distribution of $p(\overline{R},t)$

The entire finite element model of the slab has been built using the solid elements. Due to the symmetry of the slab, only ¼ of it has been modelled, with the assumption of symmetry planes and boundary conditions. The entire mesh consists of $3*10^5$ elements, and the stable time increment for Abaqus explicit algorithm was $.3*10^{-6}$ [s].

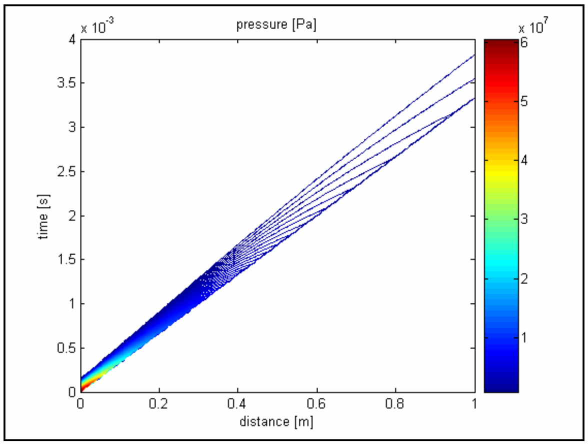

Figure 7. Contour plot of $p(\overline{R},t)$

5. Analysis of results

Both cases (0.5 and 1.0 kg of PETN charge) were analysed using the Abaqus/Explicit built-in Concrete Damaged Plasticity (CDM) default material model for concrete and the proposed material model implemented as a user subroutine (VUMAT).

Basic parameters for analysed material models are as follows:

- CDM: E = 30 GPa, $\nu = 0.19$, $\beta = 36.31$, m = 0.16, f_{b0} / f_{c0}= 1.266, K = 0.67;

Evolution of damage in compression and tension was introduced in a following form:

Compressive behavior		
Yield stress [MPa]	Inelastic strain	Damage d_c
12.5	0	0
25.0	0.00025	0.010
37.5	0.00080	0.017
40.0	0.00170	0.300
37.5	0.00370	0.440
0.50	0.01080	0.950

Tensile behavior (type = displacement)		
Yield stress [MPa]	Displacement	Damage d_t
2.90	0	0
1.95	6.61E-5	0.38
0.53	0.00048	0.98

- VUMAT:

$$E = 30\,GPa \qquad \nu = 0.19$$

$$G_f = 2500\frac{N}{m} \qquad \beta = 0.354$$

$$f_{0_{1D}}^{-} = 12.5\,MPa \qquad R_0 = \frac{f_{0_{2D}}^{-}}{f_{0_{1D}}^{-}} = 1.266$$

$$f_u^{-} = 40\,MPa \qquad f_u^{+} = f_0^{+} = 2.9\,MPa$$

$$\vartheta^{+} = 2.98 * 10^4 \qquad \vartheta^{-} = 1.36 * 10^7$$

$$a^{+} = 7.0 \qquad a^{-} = 2.0$$

The analyses were performed for a relatively long time (5 ms), in order to obtain the permanent state of damaged structure.

5.1 Test A: charge 0.5 kg PETN

First, the analysis for default CDP material model was carried out. The results are presented in Fig. 8-9, with the final distribution of damage parameters (in compression and tension) noted. The energy diagram is plotted in Fig. 10.

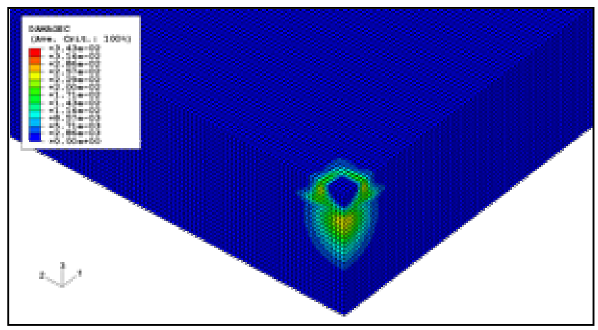

Figure. 8. Test A (0.5 kg). CDP material model. Distribution of damage parameter in compression.

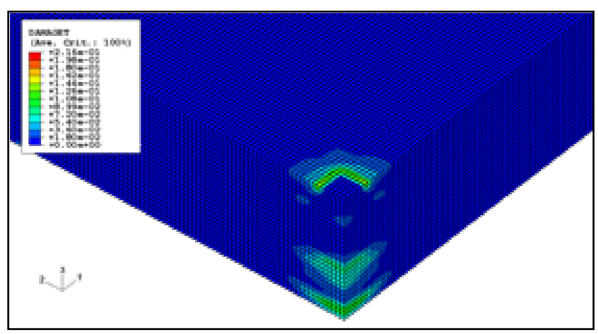

Figure. 9. Test A (0.5 kg). CDP material model. Distribution of damage parameter in tension.

Below the plot of energy versus time shows:

ALLIE – internal energy
ALLKE – kinetic energy
ALLPD – energy dissipated by plastic deformation
ALLDMD - energy dissipated by damage

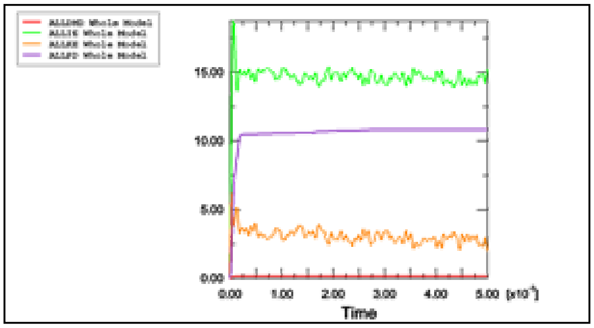

Figure. 10. Test A (0.5 kg). CDP material model. Energy plot.

Next, the analysis was conducted with the modified material model for concrete using a VUMAT subroutine.

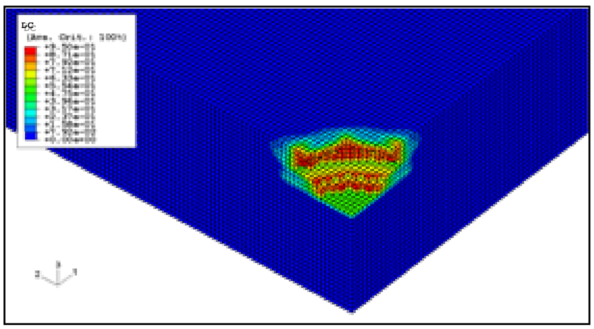

Figure. 11. Test A (0.5 kg). VUMAT material model. Distribution of damage parameter in compression. Completely damaged elements have been removed.

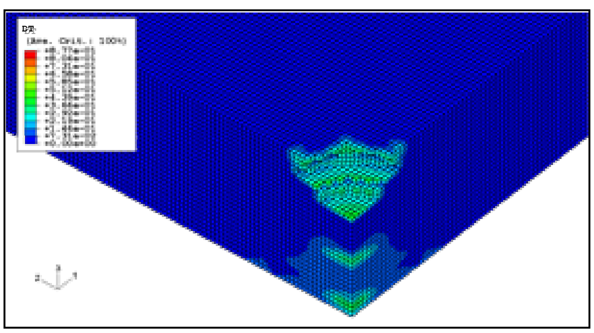

Figure. 12. Test A (0.5 kg). VUMAT material model. Distribution of damage parameter in tension. Completely damaged elements have been removed.

Comparing the results obtained using the default CDP material model and the proposed VUMAT model, one can see that the damages are much lower for the first than second model. Only in the second model (VUMAT) have damages resulting in crater formation occurred. Also, the shape (diameter and depth) of the crater is very similar to the geometry obtained experimentally (Fig. 2 and 3).

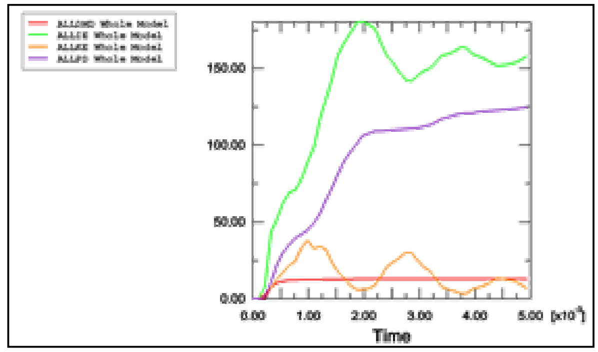

Figure. 13. Test A (0.5 kg). VUMAT material model. Energy plot.

5.2 Test B: charge 1.0 kg PETN

The results for CDP material model are presented in Fig. 14-15, with the final distribution of damage parameters (in compression and tension) noted. The energy diagram is plotted in Fig. 16.

Analogous results for assumed VUMAT material model are shown in Fig. 17-19.

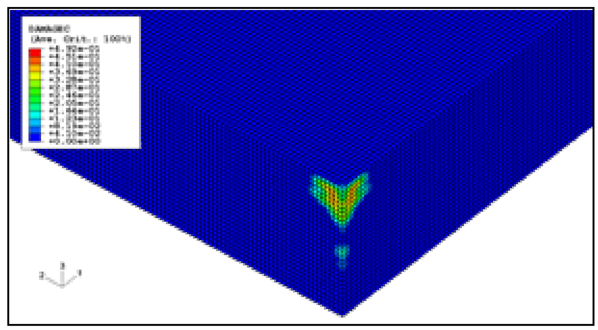

Figure. 14. Test B (1.0 kg). CDP material model. Distribution of damage parameter in compression.

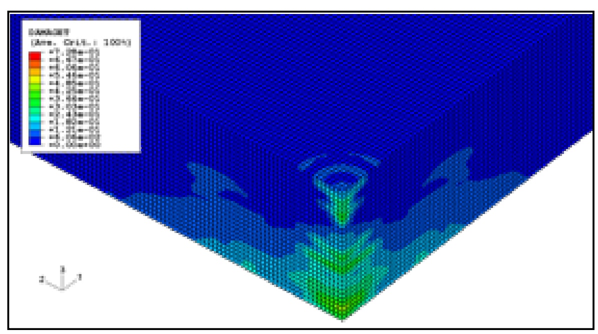

Figure. 15. Test B (1.0 kg). CDP material model. Distribution of damage parameter in tension.

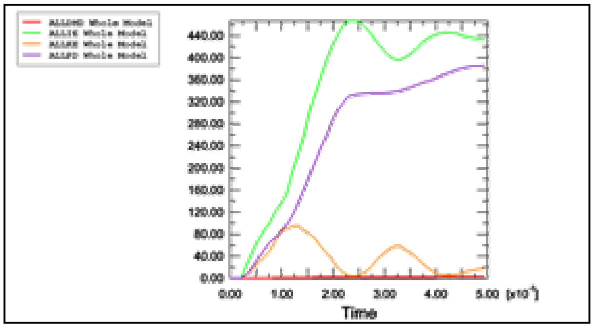

Figure. 16. Test B (1.0 kg). CDP material model. Energy plot.

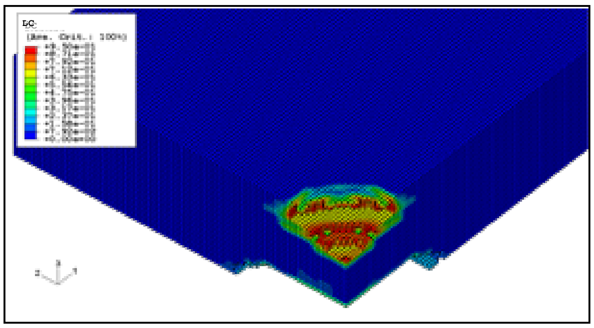

Figure. 17. Test B (1.0 kg). VUMAT material model. Distribution of damage parameter in compression.

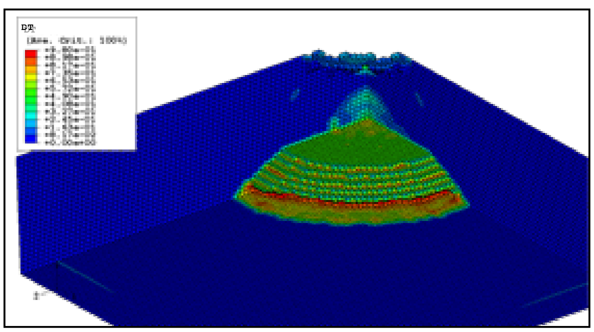

Figure. 18. Test B (1.0 kg). VUMAT material model. Distribution of damage parameter in tension.

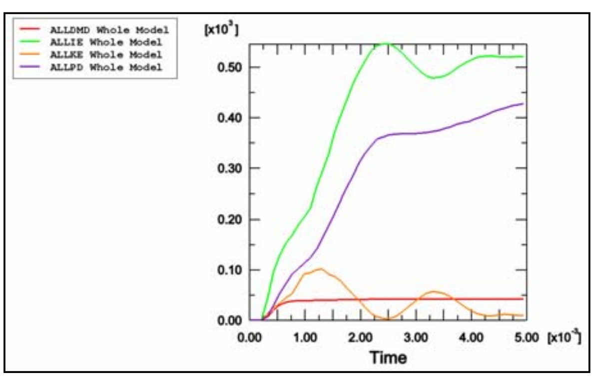

Figure. 19. Test B (1.0 kg). VUMAT material model. Energy plot.

In case B, as in case A, the comparison of numerical results obtained for two different material models shows that only for the VUMAT model has the adequate shape of both craters (upper and lower) been obtained.

6. Conclusions

The main goal of this study was to develop and implement a reliable material model for concrete into a commercial finite element computer code (Abaqus/Explicit). Although there is great variety of material models for concrete available in literature, the choice of the material formulation is difficult. The decision should take into account the physical nature of the modelled phenomenon, static or dynamic behaviour, possible rate of deformation, etc. For this reason, the relatively simple, scalar damage model has been chosen, modified, and implemented. Despite its simple formulation which neglects many important features of material behaviour under impulsive loads, the obtained results show its usefulness for practical applications.

Regarding the validation of the assumed material model, the main problem is the lack of detailed experimental data, particularly for impulsive loads of great intensity (e.g., explosions, collisions). In most cases, only the final damaged geometry of the structure is studied. With no data about the development of damages over time, the material models' calibration and verification is extremely difficult.

7. References

[1] *ABAQUS Theory Manual ver. 6.4*, ABAQUS Inc., Pawtucket, USA, 2004.

[2] Cichocki, K., Maier, G., Perego, U., Analysis of damages due to underwater explosions on a hybrid structures, *International Journal for Engineering Analysis and Design*, Vol 1, 341-361, 1994.

[3] Faria, R. and Oliver, X., *A Rate Dependent Plastic-Damage Constitutive Model for Large Scale Computations in Concrete Structures*, CIMNE, Barcelona, 1993

[4] Henrych, J., *The Dynamics of Explosions and Its Use*, Elsevier, Amsterdam, 1979.

[5] Kachanov, L.M., *Introduction to Continuum Damage Mechanics*, Martinus Nijhoff, Netherlands, 1986.

[6] Kraus, D. and Roetzer, J., A computational model for concrete structures subjected to high pressure and high strain-rates, *Proceedings of the International Conference on Computational Modelling of Concrete Structures "Euro-C"*, Innsbruck, 649-658, 1994.

[7] Mazars, J. and Pijaudier-Cabot, G., Continuum damage theory: Application to concrete. *Journal of Engineering Mechanics*, ASCE, Vol. 115(2), 345-365, 1989.

[8] Simo, J.C. and Ju, J.W., Strain- and Stress-Based Continuum Damage Models, *Int. J. Solids Structures,* Vol. 23, 821-840, 1987.

[9] Yankelevsky, D.Z., Reinhardt, H.W., Model for cyclic compressive behaviour of concrete, *J. of Struct. Eng., ASCE,* Vol. 113, 2, 228-240, 1987.

[10] Yankelevsky, D.Z., Reinhardt, H.W., Uniaxial behaviour of concrete in cyclic tension, *J. of Struct. Eng., ASCE,* Vol. 113, 2, 228-240, 1987.